Study of Nanocutting Using Atomic Model
用原子模型研究奈米切削

Chung-Ming Tan[1], Wei-Sheng Chen[1]

譚仲明 [1]，陳幃盛 [1]

[1]Graduate School of OptoMechatronics and Materials，Wufeng University

[1] 吳鳳科技大學光機電暨材料研究所

email:cmtan@mail.wfc.edu.tw

Abstract: The stress induced in a workpiece under nanocutting are analyzed by an atomic-scale model approach that is based on the energy minimization. Several aspects of the deformation evolution during the process of nanocutting are addressed. This method needs less computational efforts than traditional molecular dynamics (MD) calculations. The simulation results demonstrate that the microscopic cutting deformation mechanism in the nanocutting process can be regarded as the instability of the crystalline structure in our atomistic simulations and the surface quality of the finished workpiece varies with the cutting depth.

Keywords: nanocutting, energy minimization, deformation evolution.

摘要：基於能量最小化進行奈米切削之原子模型分析，計算工件中應力分佈。奈米切削某些方面的變形演變過程得到解釋。這種方法比傳統的分子動力學（MD）計算要簡單多。結果顯示，切削變形的微觀機制在奈米切削過程中可以看作是原子晶體結構的不穩定性，且工件表面品質隨切削深度而改變。

關鍵詞：奈米切削，能量最小化，變形演變。

Introduction

Atomistic simulations for nanocutting are employed. Belak et al. [1,2] conducted MD simulations to study the cutting of copper using the embedded-atom potential. Inamura et al. [3-6] conducted MD simulations under quasi-static conditions where only the change in the minimum energy positions is calculated. Chandrasekaran et al. [7] elucidated a formulation termed the Length Restricted Molecular Dynamics (LRMD) simulation to reduce the computational time and simultaneously decrease the memory requirements considerably. Komanduri et al. [8] conducted MD simulations of machining with large negative rake angle tools during grinding. The simulation results are in good agreement with the experimental results. Komanwduri et al. [9] investigated the effect of

tool geometry with tools of different edge radii relative to the depth of cut in nanometric cutting. Overall, although a sound foundation has been laid for the atomistic simulation of nanometric cutting, there still are many of the challenging machining problems yet to be investigated.

From the literature review presented above, it is clear that the elastic-plastic deformation that occurs during the nanocutting of a substrate is a complex phenomenon. Although this phenomenon is generally investigated using MD simulations, this technique is very time-consuming. Therefore, the present study adopts an alternative approach which is based on the fact that in condensed matters, both atoms and molecules oscillate thermodynamically around their minimum-energy positions. Under this approach, the changes in the minimum-energy positions are calculated incrementally during the cutting process. A single horizontal displacement of the tool that is used in our simulation needs more than thousands of small time-step integrations in a MD simulation. In this way, the computation becomes quasi-static, thereby yielding a significant reduction in the computation time. The objective of the present study is to provide a qualitative description of the stress and strain distributions within the copper substrate during the nanocutting process. The study also addresses the deformation mechanisms of the elastic-plastic flow and determines the influence of cutting depth upon the deformation behavior of the substrate and the quality of the finished surface of the work piece.

Mathematical Model

Figure 1 illustrates the copper atom configuration of the substrate considered in the present investigation. The arrangement of atoms can be viewed as one of a family of close-packed planes, {111}, in face-centered cubic (fcc) monocrystalline copper. In this illustration, the x-axis represents one of the families of close-packed directions, i.e. <110>. During the cutting process, a rigid sharp diamond tool is cutting into the copper substrate along the x-axis direction. The number of atoms is 4598. It is assumed that the hardness of the diamond tool far exceeds that of the copper substrate, and hence deformation of the tool can be neglected during the cutting process. The interatomic potential energy is assumed to be given by the sum of the pairwise Morse potential of the copper atoms in the substrate. This potential has the following form:

$$\phi(r_{ij}) = D\{\exp[-2\alpha(r_{ij} - r_0)] - 2\exp[-\alpha(r_{ij} - r_0)]\} \tag{1}$$

where r_{ij} is the distance between atoms "i" and "j", and copper constants D, α, and r_0 are 0.3249, 1.3588 and 2.7202, respectively. The potential between the carbon atoms of the tool and the copper atoms of the substrate is modeled by the "Born-Mayer" potential . It has the following form:

$$\phi(r_{ij}) = A\exp[-2\alpha(r_{ij} - r_0)] \tag{2}$$

where r_{ij} is the distance between carbon atom i and copper atom j, and carbon/copper constants A, α, and r_o are 0.3579, 0.9545 and 2.5, respectively.

The nanocutting process is simulated by increasing the displacements of the tool horizontally when the tool cuts the substrate at a specified depth. During the cutting process, the copper atoms in the substrate always move to their minimum-energy positions under equilibrium conditions. Hence, the nonlinear finite element formulation can be employed to establish a computationally efficient procedure to model the cutting process. In this procedure, two arbitrary atoms, "i" and "j", are regarded as two nodes, and their potential is considered to be one element. It is assumed that atom "i" is located at position (x_j, y_j) with displacements u_i and v_i in the x- and y-directions, respectively. By defining the nodal displacement vector for the "i" and "j" atoms as $\{u\}_{ij}$ and the corresponding external nodal force vector as $\{F\}_{ij} = (f_i, g_i, f_j, g_j)^T$, the total pairwise potential energy can be expressed as:

$$E_{ij} = \phi(r_{ij}) - \{u\}_{ij}^T \{F\}_{ij} \tag{3}$$

where $\phi(r_{ij})$ is the potential function between the two atoms, and the superscript "T" represents the transpose of a matrix.

By applying the principle of minimum potential energy, as the forces of the particles in a given system reach equilibrium, the particles will move to positions of minimum energy. The positions of minimum energy can be found by differentiating the total potential energy, E_{ij}, with respect to $\{u\}_{ij}$. Consequently, the limits of E_{ij} can be obtained as:

$$\frac{\partial E_{ij}}{\partial \{u\}_{ij}} = \left(\frac{\partial \phi}{\partial r_{ij}}\right)[B]^T - \{F\}_{ij} = \{0\} \tag{4}$$

Equation (4) is the element equilibrium equation, in which suffixes "i" and "j" denote two arbitrary atoms. Equation (4) can be assembled to obtain the equilibrium equation for the whole system, i.e.

$$\sum_{i \neq j}\left(\frac{\partial \phi}{\partial r_{ij}}\right)[B]^T - \{F\}_{ij} = \{f\}_{\text{internal}} - \{F\}_{external} = \{0\} \tag{5}$$

In terms of the finite element formulation, Equation (11) represents the tangent stiffness equation, while the terms $\{f\}_{\text{internal}}$ and $\{F\}_{external}$ in Equation (5) denote the internal force vector and the external force vector, respectively.

Results and Discussion

Figure 1 (c) presents the configuration of the substrate after cutting. As can be seen, several slips orientated at approximately 60° to the horizontal direction are propagated from the finished surface. This is to be expected since slip generally occurs along the

closed-packed directions. This observation indicates that the most fundamental plastic deformation mechanism takes place during the nanocutting process. The slips occur as the result of the nucleation and propagation of dislocations. By neglecting the thermal vibrations of the atoms, the present study transforms the MD formulation into a static finite element structural problem. Therefore, the stability of the crystalline structure can be monitored by the non-positiveness of the tangent stiffness matrix, K_t, of the present finite element formulation. The irreversible plastic deformations observed in the simulation, i.e. slips, can be considered to be the consequence of changes in the crystalline structure caused by instabilities induced by high localized stresses [10,11]. From Figure 1(b), it can be deduced that series localized instabilities of the substrate crystal structure cause the cutting force versus cutting distance curve to fluctuate violently, i.e., each cutting force drop denotes the nucleation and propagation of dislocations induced by the instabilities. The von Mises stress and the hydrostatic stress distributions corresponding to the deformed configuration of Figure 1 (c) are presented in the contour subplots of Figure 2 (a) and (b). A comparison of the von Mises stress and hydrostatic stress distributions suggests that the dilatation or compression of the substrate is mostly recovered beneath the finished surface. In contrast, it is also noted that a large part of the distortion of the substrate appears to be permanent. Hence, the change of the crystalline structure caused by the high localized stresses tends to result in distortion of the substrate. Furthermore, it can be seen that the nanocutting process induces high residual stresses, which by definition remain within the substrate once the tool has cut through.

To observe the nucleation and glide of dislocations more clearly, several indices of characterizing the deformation in an atomistic model are presented in Figures 2 (c) and (d). Corresponding to figure 1 (c), Figure 2 (c) and (d) representing x component and y component of slip vector can characterize the deformation of slip of atoms most precisely. This is easily to understand due to the closed-packed directions are 60 ° or 120 ° from the horizon.

A well-known phenomenon for large-scale metal cutting is that the residual stress of the finished surface detriments the durability of the machined work piece. Therefore, three subplots are shown in Figure 3 (a), (b) and (c) to present the distributions of von Mises stress for three different cutting depths 0.1, 0.15 and 0.2 nm. Observing the three subplot in Figure 3 (a), (b) and (c), it can be seen that there is larger region of high residual stress in the finished surface as the cutting depth increases.

Smooth finished surface is commonly expected for cutting machining. From the slip vector analysis in the previous section, we observed dislocations emitted from the finished surface that correlate with the roughness of the surface. Therefore, three subplots are shown in Figure 3 (d), (e) and (f) to present the distributions of y component of slip vector for three different cutting depths 0.1, 0.15 and 0.2 nm. Observing the three subplot in

Figure 3 (d), (e) and (f), it can be seen that there are more dislocations propagated from the finished surface as the cutting depth increases.

Conclusions

The current simulations of the nanocutting process adopt a nonlinear finite element formulation which ignores the thermal vibrations of atoms in the condensed matter, and hence enables a more computationally efficient approach for modeling the deformation evolution of the substrate during nanocutting than the conventional molecular dynamics simulation method. The major findings of the present study may be summarized as follows:

(1)   The current static finite element structural analysis indicates that plastic deformation of the substrate is the consequence of the instability of the crystalline structure of the substrate. Furthermore, the occurrence of this instability can be monitored by the non-positiveness of the tangent stiffness matrix of the crystalline structure.

(2)   The fundamental plastic deformation mechanism is evident in the present simulation results, namely slips. Slips are caused by the nucleation and propagation of dislocations.

(3)   The quality of the finished surface in the work piece detriments with the increasing cutting depth.

References

[1]   J. Belak, I.F. Stowers, A molecular dynamics model of the orthogonal cutting process, in: Proc. ASPE Annu. Conf.,1990, p. 76, Rochester, NY.

[2]   J. Belak, D.A. Lucca, R. Komanduri, R.L. Rhorer, T. Moriwaki, K. Okuda, S. Ikawa, S. Shimada, H. Tanaka, T.A. Dow, J.D. Drescher, I.F. Stowers, Molecular dynamics simulation of the chip forming process in single crystal copper and comparison with experimental _ . data, Proc. ASPE Annu. Conf. 1991 100.

[3]   T. Inamura, H. Suzuki, N. Takezawa, Cutting experiments in a computer using atomic models of copper crystal and a diamond tool,   Int. J. Jpn. Soc. Precis. Eng. 25 4 1991 259.

[4]   T. Inamura, N. Takezawa, N. Taniguchi, Atomic-scale cutting in a computer using crystal models of copper and diamond, Ann. CIRP. 41 1 1992 121.

[5]   T. Inamura, N. Takezawa, Y. Kumaki, Mechanics and energy dissipation in nanoscale cutting, Ann. CIRP 42 1 1993 79.

[6]   T. Inamura, N. Takezawa, Y. Kumaki, T. Sata, On a possible mechanism of shear deformation in nanoscale cutting, Ann. CIRP 43 1 1994 47.

[7]   N. Chandrasekaran, A. Noori-Khajavi, L.M. Raff, R. Komanduri, A new method for molecular dynamics simulation of nanometric cutting, Philos. Mag. B 77 1 1998 7.

[8]   R. Komanduri, N. Chandrasekaran, L.M. Raff, Some aspects of machining with

negative rake tools simulating grinding: an MD simulation approach, Philos. Mag. B 79 7 1999 955.

[9] R. Komanduri, N. Chandrasekaran, L.M. Raff, Effect of tool geometry in nanometric cutting: an MD simulation approach, Wear 219 1998 84.

[10] M. F. Horstemeyer, M. I. Baskes, A. Godfrey, D. A. Hughes, "A Large Deformation Atomistic Study Examining Crystal Orientation Effects on the Stress-Strain Relationship," Int. J. Plast.18 2002, pp. 203-229.

[11] Y. R. Jeng, and C. M. Tan, "Theoretical Study of Dislocation Emission around a Nanoindentation Using a Static Atomistic Model," Phys. Rev. B 69 2004, 104109.

(a)

(b)

(c)
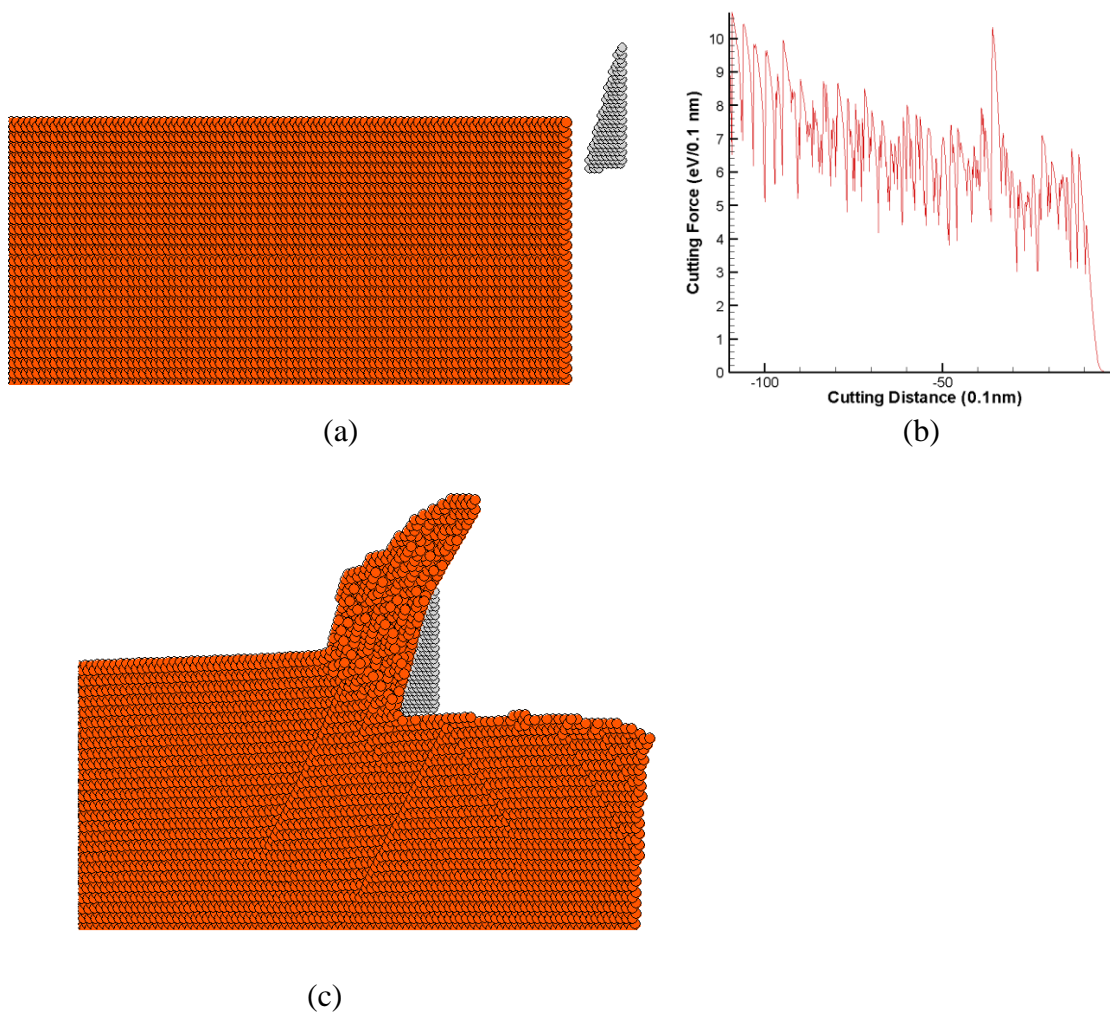
Figure 1 (a) Atomistic model used in present nanocutting simulation.(b) Cutting force versus cutting distance curve. (c) Configuration of deformed substrate during nanocutting process.
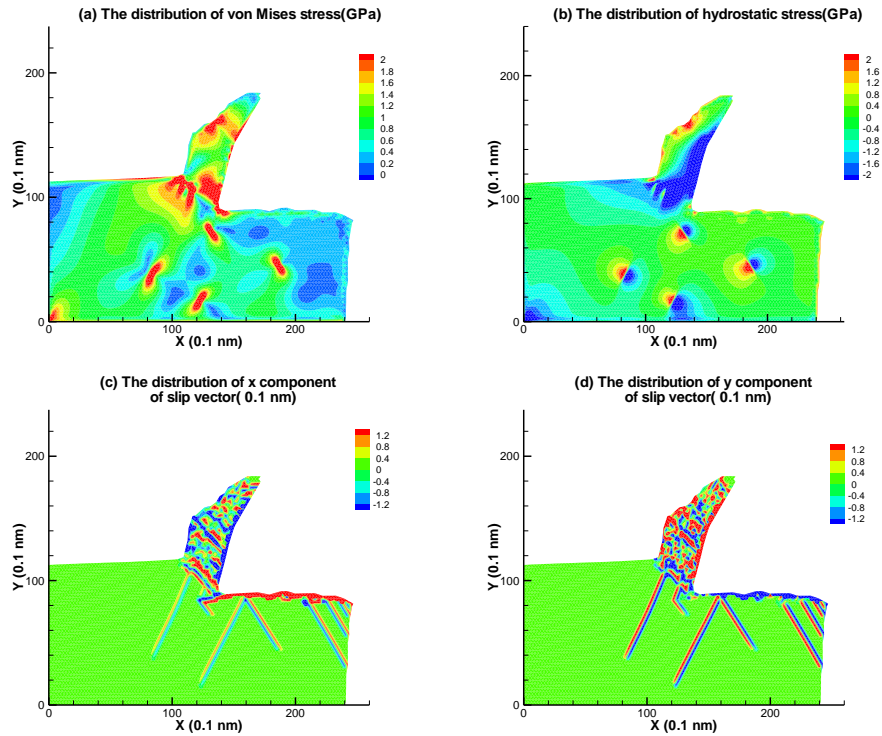
Figure 2 Flooded contour subplots of von Mises stress and hydrostatic stress distributions corresponding to the deformed configuration in Figure 2 (a) and (b). Flooded contour subplots of the distribution of x component and y component of slip vector in Figure 2 (c) and (d).
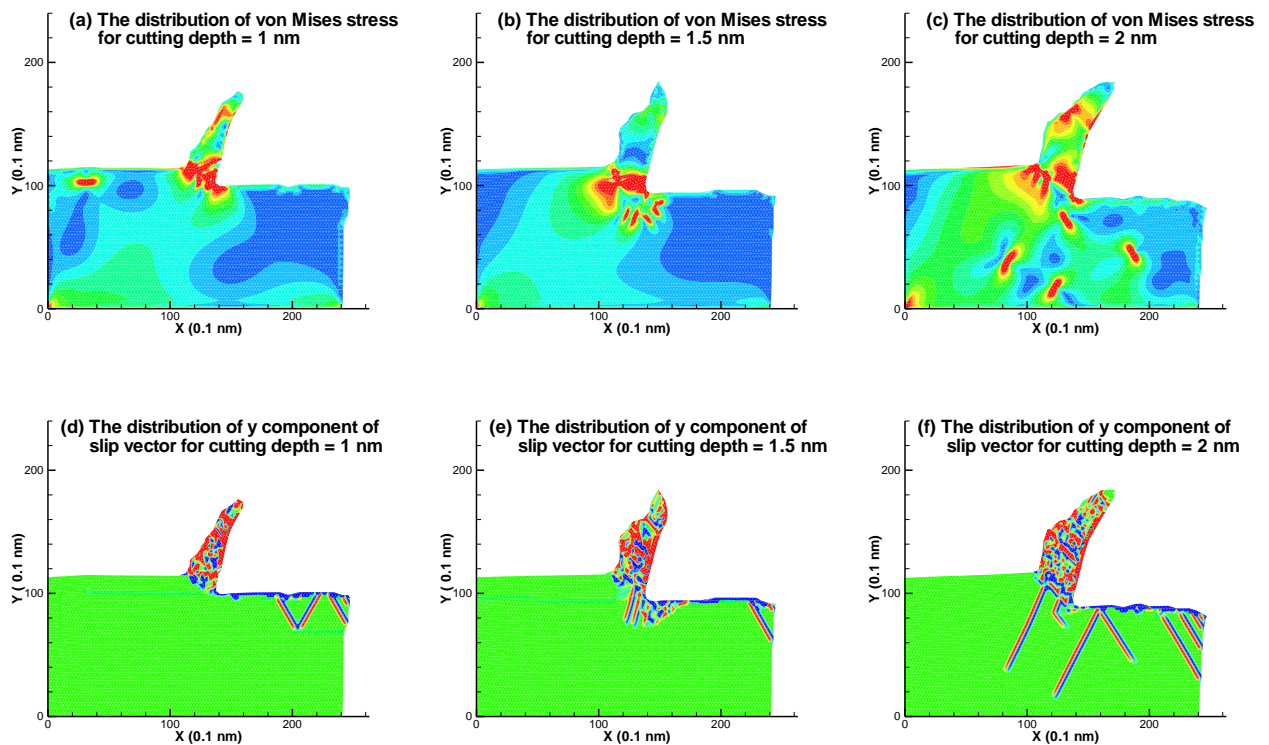
Figure 3 Flooded contour subplots of von Mises stress distributions corresponding to three differentcutting depths 0.1 nm, 0.15 nm and 0.2 nm in Figure 3 (a), (b) and (c). Flooded contour subplots of the distribution of y component of slip vector corresponding to three different cutting depths 0.1nm, 0.15 nm and 0.2 nm in Figure 3 (d), (e) and (f).